Magazine of Civil Engineering

ISSN 2712-8172

journal homepage: http://engstroy.spbstu.ru/

DOI: 10.18720/MCE.99.9

Bending torsion in Γ-shaped rigid and warping hinge joints

V.A. Rybakov*[a], D.O. Sovetnikov[b], V.A. Jos[a]

[a] *Peter the Great St. Petersburg Polytechnic University, St. Petersburg, Russia*

[b] *Bryden Wood Technology Ltd, London, United Kingdom*

** E-mail: fishermanoff@mail.ru*

Keywords: lightweight gauge steel structures, warping hinge, plane frame, thin-walled rods, Slivker's semi-shear theory, rigid joint, bimoment, warping

Abstract. This paper investigates the effect of bending torsion which is the cross-sectional warping of thin-walled rods at plane frame joints in the framework of the "semi-shear" theory of V.I. Slivker. Studied are the shell finite element models of rigid and "warping hinge" joints in thin-walled bar structures, designed and calculated in the software package Ansys Workbench. The correlation of the geometric characteristics of thin-walled profiles and the connecting plate is considered towards the change in the value of normal stresses and bimoments when the cross-sectional axis is rotated. The obtained ratios of the bimoment stresses before and after the rotation of the cross-sectional axis of the joints are presented. The study concentrates the distribution of the bimoments and warpings in the plane frame with rigid joints with and without the consideration of the coefficient of the cross-sectional axis rotation. The comparison of the obtained results for both cases is shown.

1. Introduction

This article is an extended version of the report presented on the International Scientific Conference on Energy, Environmental and Construction Engineering (EECE 2019) [1].

Nowadays thin-walled systems play a significant role in the civil engineering industry. This technology has a wide range of applications in the construction. The development of light gauge steel structures (LGSS) counterbalanced by the insufficiently research-supplied normative documents awakes interest in the scientific world and challenges engineers and scientists to take efforts in order to establish the most rational and universal methods of design for such structures. In recent years there have been dozens of publications concerning different types of problems.

Today, one of the most applicable and appropriate approaches in the design and analysis of thin-walled systems is the «semi-shear» theory of V.I. Slivker, which was firstly published in [2]. In the framework of this theory V. Lalin et al. developed the cycle of numerical methods, concerning the stiffness matrices of various thin-walled finite elements [3, 4].

The variational formulations and the finite element method are the fundamental issues of the analysis of the structures [5, 6]. The finite element analysis of the thin-walled cold-formed Z-purlins supported by sandwich panels using finite elements in the software package MSC Nastran were described by O. Tusnina [7, 8]. The numerical examples in the framework of the problems of geometrically nonlinear dynamic analysis based on the corotational finite element formulation were presented in [9].

The study [10] proposed the methods of parametric optimization of thin-walled structures together with presenting the results of this optimization.

There were several papers dealing with the finite element models of cold-formed thin-walled steel profiles with solid and slotted webs. The papers [11, 12] presents results of numerical experiments about elastic shear buckling and ultimate shear strength. The derived equations demonstrate high accuracy results compare to the finite element simulation results. More detailed numerical parametric study concerning cold-formed thin-walled steel profiles was conducted in [13, 14], where the different geometric parameters and types of boundary conditions were varied in order to understand their influence on stress-strain state of the

constructions. The effects of boundary conditions on the elastic shear buckling load and the ultimate shear strength were investigated.

The buckling analysis of thin-walled steel frames with rigid joints based on the Generalised Beam Theory (GBT) was performed in [15, 16]. The shell finite element models were designed in the program package ANSYS to conduct analysis. One of the goals of these studies was simulating the warping transmission at frame joints connecting two or more members using a GBT-based beam finite element. Based on the same theory the post-buckling analysis of the thin-walled L-shaped frames and symmetric portal frames was studied in [17]. For validation proposes, most analytical results were compared to the numerical values obtained in the program package. The GBT-based (beam) finite elements were applied by authors of [18]. These finite elements were combined with the shell finite elements in order to propose a general and efficient approach to model thin-walled members with the sophisticated geometries and/or connected through joints. To validate the obtained results full shell finite element model solution were presented, confirming the high accuracy and excellent match.

The describing of the buckling of thin-walled structures was shown in [19]. This paper studies the buckling of the thin-walled two bar frame, loaded by a dead force at the joint. Various warping constraints at the bar ends are considered and the relevant buckling modes and loads are numerically evaluated.

The influence of the rotational stiffness of the beam to column connection on the strength and the stability of thin-walled structure was considered in [20]. The surrogate models and the basic techniques of their construction to calculate initial rotational stiffness of welded rectangular hollow section (RHS) joints were discussed in study [21]. Rectangular hollow section T-joints were vastly investigated in the context of axial and initial in-plane rotational stiffnesses, employing finite element modelling in order to test the existing calculation approaches; new equations, describing the chord stress behavior were derived and validated as well [22, 23].

There were investigated some methods of solving problems of bending torsion avoiding sophisticated calculational process [24]. The suggested formula makes it possible to calculate the bimoment using the previously known values of the bending moment and the eccentricity of the applied load. The paper [25] focused on the determination of the torsional characteristics. These parameters plays a significant role in the process of design of members subjected to the bending with respect to lateral torsional buckling.

Also, it is important to note that one of the core problems in creation of a universal algorithm for calculating random thin-walled rod systems is the determination of boundary conditions in joints.

One of the approaches aiming at the consideration of the boundary conditions on the ends of thin-walled rods neglects the warping of them [26]. The hypothesis within the framework of the A.R. Tusnin theory is that the warping is equal for each rod intersecting in a joint [27, 28].

The work of V.V. Yurchenko and M.A. Perelmuter disproves the Tusnin theory and states that the warping is different for each intersecting rod and does not have any dependencies [26].

The goal of the present work is the analysis of the stress-strain state of shell finite element models of the rigid and «warping hinge» joints designed in the software package Ansys Workbench and the search for the approach, considering the warping in terms of the stress transition from one element to the other in the rigidly connected plane frame joints within the framework of the V.I. Slivker theory.

Object of the research is thin-walled plane bar systems.

Subject of the research is the stress-strain state of thin-walled plane bar systems under the transverse bending load with an eccentricity.

2. Methods

The computational model is considered to be the Г-shaped joint of a plane frame, made of thin-walled profiles.

The following symbol is introduced for further reference.

K_ω is the coefficient of the cross-sectional axis rotation that characterizes the ratio of bimoments in cross-sections on each side of the joint:

$$K_\omega = \frac{B_2}{B_1} \tag{1}$$

where B_1 is the value of the bimoment in the cross-section of the loaded thin-walled member; B_2 is the value of the bimoment in the cross-section of the load-free member.

The ratio of bimoments in the joint cross-section is equal to the ratio of the normal stresses:

$$\sigma_i = \frac{N}{A} + \frac{M_y}{I_y} z_i + \frac{M_z}{I_z} y_i + \frac{B}{I_\omega} \omega_i \quad (2)$$

It is known from literature review [2, 9, 28] that tangential stresses, appearing in the cross-sections of the joint elements, are considerably (more than 10 times) lower than normal stresses – the effect is negligible. Longitudinal force is not applied to the elements, therefore, for the estimation of the bimoments only normal stresses are accounted for:

$$\sigma \sim \frac{B}{I_\omega} \omega \to K_\omega = \frac{B_2}{B_1} = \frac{\sigma_2}{\sigma_1} \quad (3)$$

This paper investigates 3 different shell finite element models of joints in bar structures. One of them represents a rigid joint, and others are the so-called «warping hinge» joints (Fig. 1). Under “warping hinge” a bar fixation which does not correspond to the rotation of the support cross-section is assumed (the cross-section is fixed against rotation of the longitudinal axis), wherein the cross-section can get freely warped out of its plane (sectorial longitudinal forces (bimoment) are not present). This definition was firstly introduced in [29]. These models were designed and calculated in the software package Ansys Workbench.

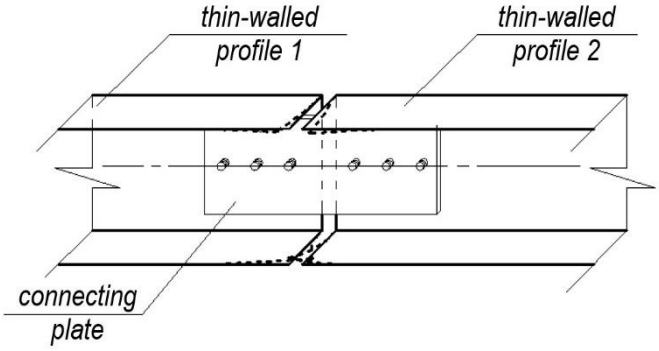

Figure 1. “Warping hinge”.

2.1. Rigid joint

The Table 1 provides main geometric parameters of the rigid joint corresponding to the Standards of the Organization 83835311.001–2015 (Russia).

Table 1. Geometric parameters of the rigid joint.

Characteristics		Value	Unit of Measurement
Basic dimensions of the profile		200×50×1.5	mm
Length of the “beam”		105	mm
Length of the “column”		450	mm
Basic dimensions of the connecting plate		300×300×6	mm
Steel density	ρ	7858	kg/m^3
Young's modulus	E	$2 \cdot 10^{11}$	Pa
Poisson’s ratio	ν	0.3	mm

The rigid joint is a Г-shaped joint (Fig. 2), made of two thin-walled profiles with identical cross-sections wherein the corresponding flanges of the “beam” and “column” are extended to each other. The “beam” and “column” are rigidly assembled by non-thin connecting plate. The connection between the cross-sections of the “beam” and “column” are considered firm during the calculation. The bottom of the “column” in all of the cases is rigidly fixed.

The applied load is linearly distributed over the flanges of the cross-section simulating the action of the bimoment. The load is applied to the nodes of the finite elements (Fig. 3). The modulus of the maximum magnitude of the applied linearly distributed load is equal to 1000 N.

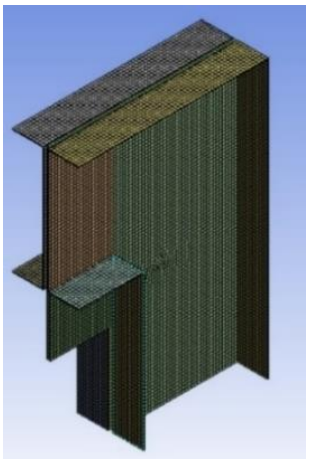

Figure 2. Finite element model of the rigid joint.

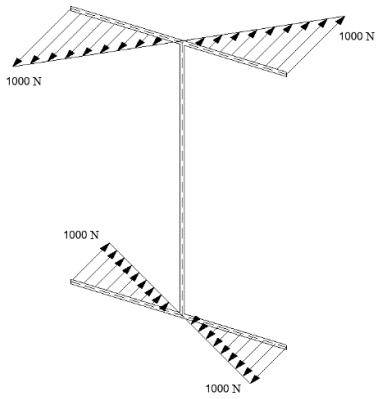

Figure 3. Applied load.

Researched are the normal stresses in the cross-sections of the “beam” and “column” one finite element (5 mm) away from the connecting plate under different parameters:

1. The thickness of the connecting plate;
2. The linear dimensions of the connecting plate;
3. The thickness of thin-walled profiles.

Table 2. Value of the coefficient of the rotation with varying connecting plane thickness for the rigid joint.

	Normal stresses in the “beam”, MPa						Normal stresses in the “column”, MPa						$\frac{\overline{\sigma_b^1}}{\overline{\sigma_b^2}}=\frac{B_1}{B_2}$	$\frac{\overline{\sigma_t^1}}{\overline{\sigma_t^2}}=\frac{B_1}{B_2}$
	σ_{C1}^1	σ_{D2}^1	σ_{A1}^1	σ_{B2}^1	$\overline{\sigma_b^1}$	$\overline{\sigma_t^1}$	σ_{B1}^2	σ_{D2}^2	σ_{A1}^2	σ_{C2}^2	$\overline{\sigma_b^2}$	$\overline{\sigma_t^1}$		
Connecting plate 300x300 mm	bottom	bottom	top	top	top (average)	top (average)	bottom	bottom	top	top	bottom (average)	top (average)	bottom/bottom	top/top
t = 4 mm	-28.673	-28.673	28.674	28.674	28.673	28.674	6.5926	6.5926	-5.3649	-5.3649	6.5926	-5.3649	4.349	5.345
t = 6 mm	-28.675	-28.675	28.675	28.675	28.675	28.675	5.5515	5.5515	-5.0338	-5.0338	5.5515	-5.0338	5.165	5.696
t = 8 mm	-28.679	-28.679	28.676	28.676	28.679	28.676	3.9542	3.9542	-3.9935	-3.9935	3.9542	-3.9935	6.346	6.665

Table 2 contains the normal stresses in the «beam» and «column» in the case of the unchanging cross-section of the thin-walled profile 200×50×1.5 mm and the plate with lineal dimensions 300×300 mm with varying connecting plane thickness (t = 4 mm, t = 6 mm, t = 8 mm) for the rigid joint. The numbering of cross section points is shown in the Fig. 4, Fig. 5.

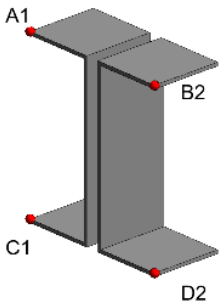

Figure 4. Calculational points in the "beam".

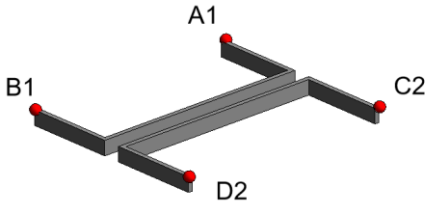

Figure 5. Calculational points in the "column".

The obtained ratios of the bimoment stresses before and after the rotation of the cross-sectional axis of the rigid joint are reflected in the Table 3.

The graphs of the influence of the various geometric characteristics on the ratio of the normal stresses/bimoments for the rigid joint are shown in Fig. 6, Fig. 7, Fig. 8.

Table 3. Ratio of bimoment stresses in the "beam" and "column" cross-sections, depending on different geometric factors for the rigid joint.

	Profile 200×50×1.5 mm						Connecting plate 300×300×6 mm		
	Connecting plate 300×300 mm			Connecting plate t = 6 mm			Profile 250×50 mm		
	t = 4 mm	t = 6 mm	t = 8 mm	250×250 mm	300×300 mm	350×350 mm	t = 1 mm	t = 1.5 mm	t = 2 mm
σ bottom/bottom	4.35	5.17	6.35	4.79	5.17	5.08	5.61	5.17	5.00
σ top/top	5.34	5.70	6.67	6.67	5.70	5.42	5.84	5.70	5.83

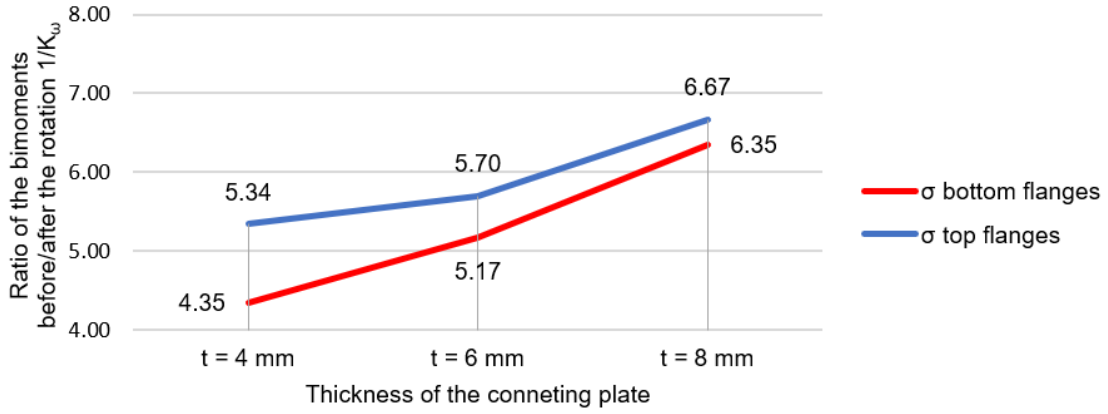

Figure 6. Dependence graphs of the bimoment change on the connecting plate thickness for the rigid joint.

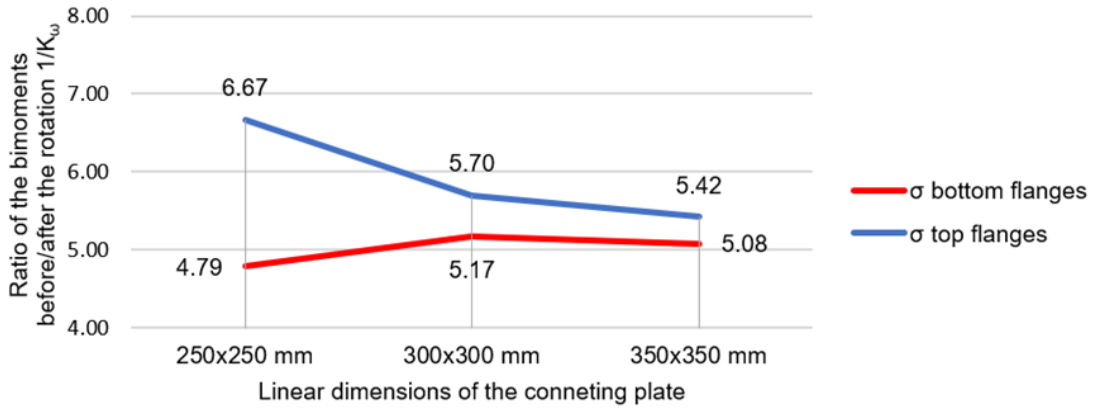

Figure 7. Dependence graphs of the bimoment change on the connecting plate linear dimensions for the rigid joint.

Figure 8. Dependence graphs of the bimoment change on the thin-walled profiles thickness for the rigid joint.

Based on the obtained results, the next conclusions were made:

1. The ratio of the normal stresses/bimoments before/after the rotation of the cross-sectional axis of the rigid joint are compatible for the top and bottom flanges;

2. The change of the normal stresses and bimoments of the rigid joint with varying connecting plane thickness has a linear dependence;

3. The change of the normal stresses and bimoments of the rigid joint with varying linear dimensions of the connecting plate has the linear dependence for the top flanges of the cross-section and has a constant value for the bottom flanges of the cross-section;

4. The change of the thickness of thin-walled profiles of the rigid joint has a negligible contribution to the value of normal stresses/bimoments before and after the rotation of the cross-sectional axis.

2.2. "Warping hinge" joints

The paper investigates two configurations of the "warping hinge" connection. The Configuration 1 represents a Г-shaped node of two thin-walled profiles of the same cross-section firmly assembled by non-thin connecting plate (Fig. 10). The Configuration 2 is a Г-shaped node of two thin-walled profiles of the same cross-section wherein the upper point of the "column" coincides with the level mark of the upper "beam" shelf (Fig. 11).

The connection between the flanges is not considered while the calculations – the connection represents the so-called "warping hinge" joint, which is achieved by the spacing one finite element wide (5 mm) in-between the flanges. Since the flanges of the "column" and the "beam" are not connected to each other, the connection is realized through the webs, the flanges can get freely warped out of their planes (there are no normal stresses on the ends of the flanges because the ends of the flanges are not loaded with bimoment or other axial loads). The Fig. 9 demonstrates the distribution of sectorial coordinates, which justifies the applicability of the selected models for calculation [30]. According to the graph it is clear that values along the web are equal to zero.

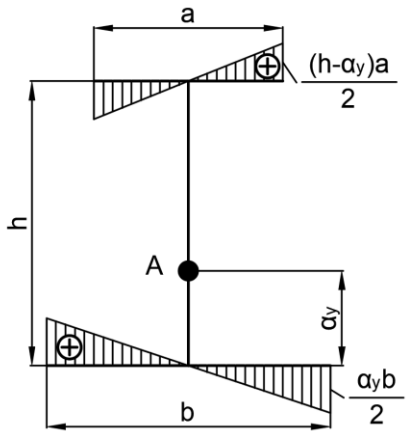

Figure 9. Distribution of sectorial coordinates.

The Table 4 demonstrates general geometric characteristics of the "warping hinge" joints corresponding to the Standards of the Organization 83835311.001–2015 (Russia).

Table 4. Geometric parameters of the "warping hinge" joint.

Characteristics			Value	Unit of Measurement
Basic dimensions of the profile			200×50×1.5	mm
Length of the "beam"			105	mm
Length of the "column"	Configuration 1		250	mm
	Configuration 2		450	
Basic dimensions of the connecting plate			300×300×6	mm
Steel density		ρ	7858	kg/m^3
Young's modulus		E	$2 \cdot 10^{11}$	Pa
Poisson's ratio		ν	0.3	mm

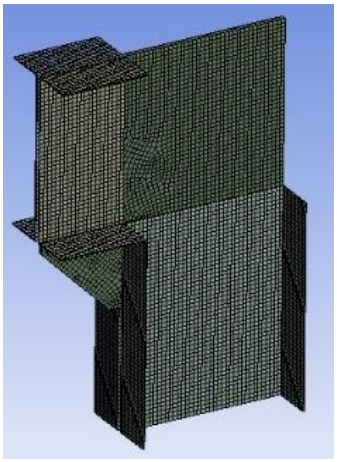

Figure 10. Finite element model of the "warping hinge" joint (Configuration 1).

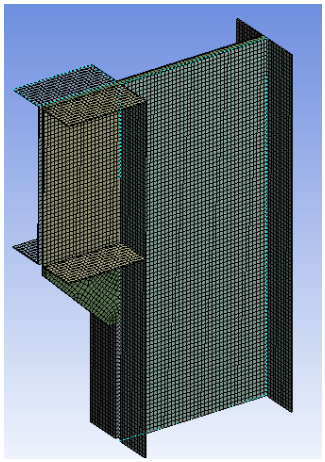

Figure 11. Finite element model of the "warping hinge" joint (Configuration 2).

The applied load has an equal value and character as it was realized with the rigid joint.

The whole algorithm of analyzing the "warping hinge" models is the same as for the rigid joint. Researched are the normal stresses in the cross-sections of the "beam" and "column" one finite element (5 mm) away from the connecting plate in the Configuration 1 and in the same points in the Configuration 2 under different parameters.

The obtained ratios of the bimoment stresses before and after the rotation of the cross-sectional axis of the "warping hinge" joints are reflected in the Table 5.

The graphs of the influence of the various geometric characteristics on the ratio of the normal stresses/bimoments for the "warping hinge" connections are shown in Fig. 12, Fig. 13, Fig. 14.

Table 5. Ratio of bimoment stresses in the "beam" and "column" cross-sections, depending on different geometric factors for the "warping hinge" joints.

	Profile 200×50×1.5 mm						Connecting plate 300×300×6 mm		
	Connecting plate 300×300 mm			Connecting plate t = 6 mm			Profile 250×50 mm		
	t = 4 mm	t = 6 mm	t = 8 mm	250x250 mm	300x300 mm	350x350 mm	t = 1 mm	t = 1.5 mm	t = 2 mm
Configuration 1									
σ bottom/bottom	9.58	11.13	13.38	10.51	11.13	11.65	12.22	11.13	10.62
σ top/top	12.68	12.67	14.44	14.04	12.67	12.81	12.70	12.67	13.15
Configuration 2									
σ bottom/bottom	5.58	5.93	7.98	4.75	5.93	7.10	6.56	5.93	6.36
σ top/top	5.52	6.40	7.93	4.74	6.37	7.54	6.51	6.40	6.30

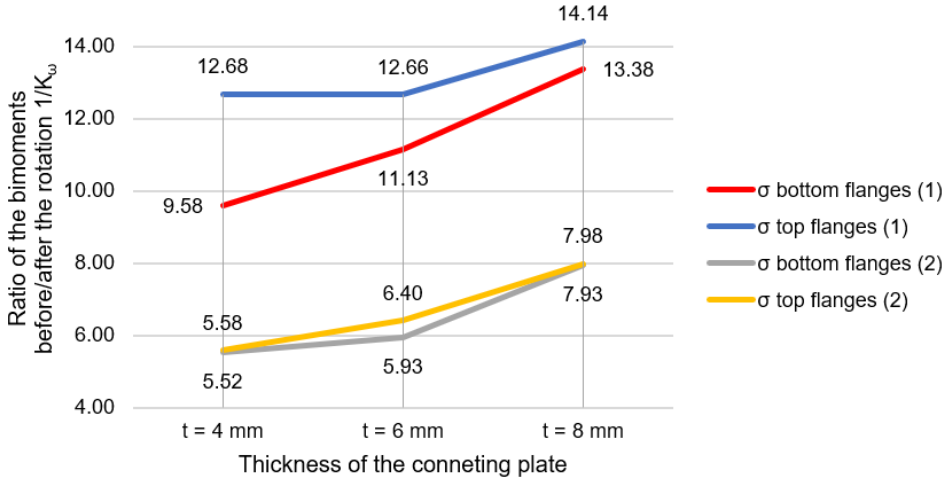

Figure 12. Dependence graphs of the bimoment change on the connecting plate thickness for the "warping hinge" joints.

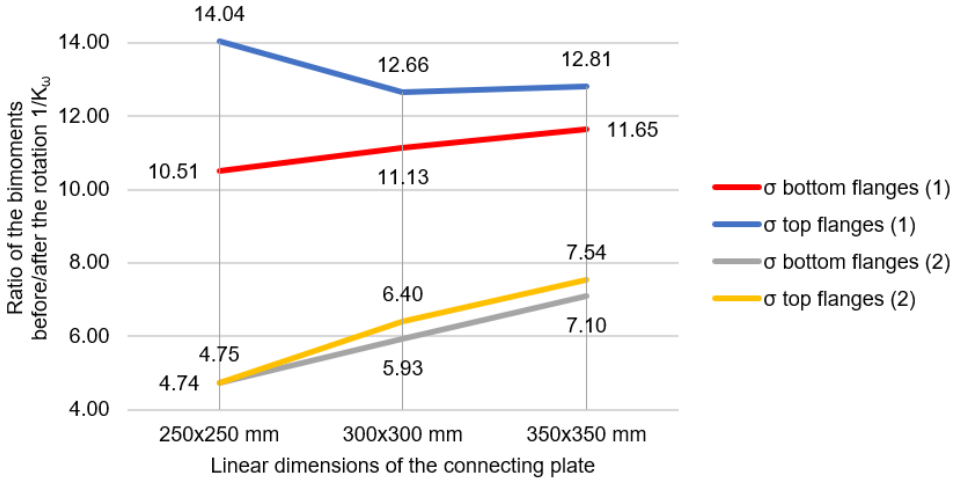

Figure 13. Dependence graphs of the bimoment change on the connecting plate linear dimensions for the "warping hinge" joints.

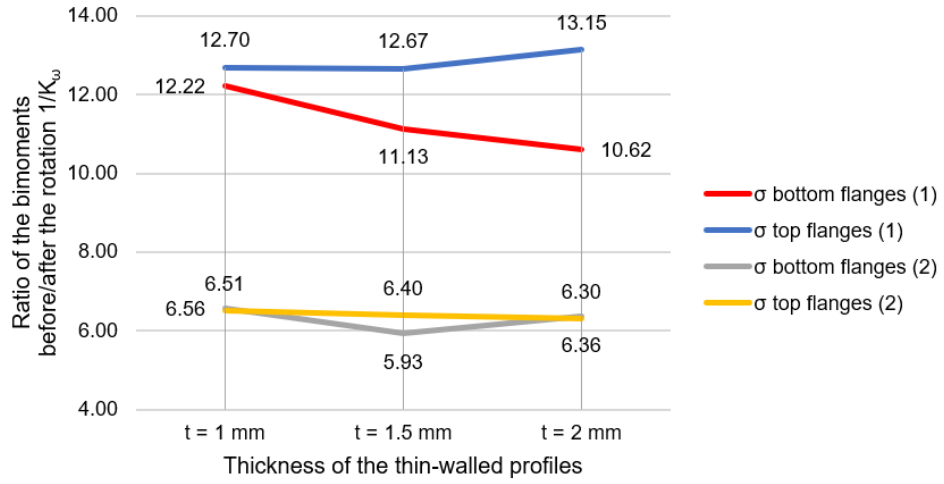

Figure 14. Dependence graphs of the bimoment change on the thin-walled profiles thickness for the "warping hinge" joints.

Based on the obtained results the following conclusions can be drawn:

1. The reduction coefficient should be regarded when the rotation of the axis of the "warping hinge" in considered;

2. The relation between the normal stresses/bimoments before/after the rotation of the cross-sectional axis in case of the Configuration 1 has a divergence for low and upper flanges of more than 15 %. For the Configuration 2 these ratios have approximately the same values;

3. The change of normal stresses and bimoments under different geometrical characteristics of the connecting plate (when measuring the thickness and linear dimensions) has a linear dependency in case of "warping hinge" connection;

4. The change in the profile thickness does not have a significant influence on the ratio between the normal stresses/bimoments before/after the rotation of the cross-section.

3. Results and Discussion

Within the framework of the Tusnin theory [26] the rotation cosine of the warping measure is equal to 1, which means that the warping does not depend on the coordinate system.

For the comparison with the Tusnin theory let us assume the bimoment to be a conditional vector, rotation angle cosine of which is define as a ratio of the bimoment after the rotation of the structure axis to the bimoment before the rotation (i.e. instead of 1 assume the value of the coefficient K_ω).

The computational model is the frame consisting of three bars (Fig. 15). The length of columns is 4 m, the length of the crossbar is 6 m. The calculation was performed in the software Maple. The parameters of the bar cross-section are taken as for the coupled out of two thin-walled profiles PN200–50–1.5 (Fig. 16).

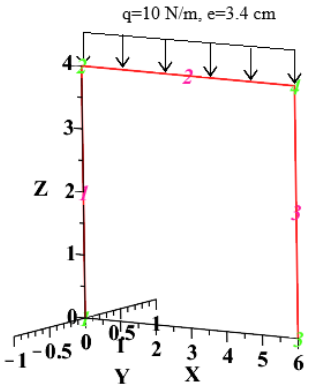

Figure 15. Computational model in Maple.

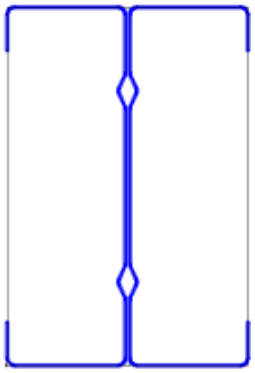

Figure 16. Coupled profile PN200–50–1.5.

Below are the graphs of the distribution of the bimoments and warpings along the columns and the crossbar for the rigid joint without considering the coefficient K_ω (Fig. 17, Fig. 19).

Further the K_ω is assumed as for the rigid connection with the value of 0.184. This value of the coefficient is referred to as the cosine of the rotation and is exceptionally applied to two finite column elements, adjacent to the crossbar.

Graphs of the distribution of the bimoments and warpings along the columns and the crossbar for the rigid joint with the coefficient $K_\omega = 0.184$ are presented below (Fig. 18, Fig. 20).

For the calculation with the rotation coefficient the obtained bimoments are neglected on the ends of the columns, adjoint to the crossbar, since the area is within the joint connection.

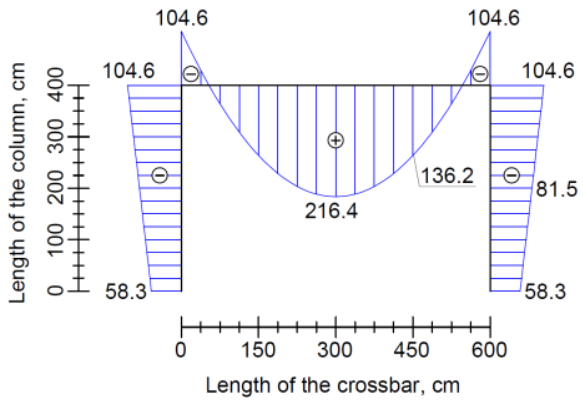

Figure 17. Distribution of the bimoment (daN·cm²) without considering the K_ω.

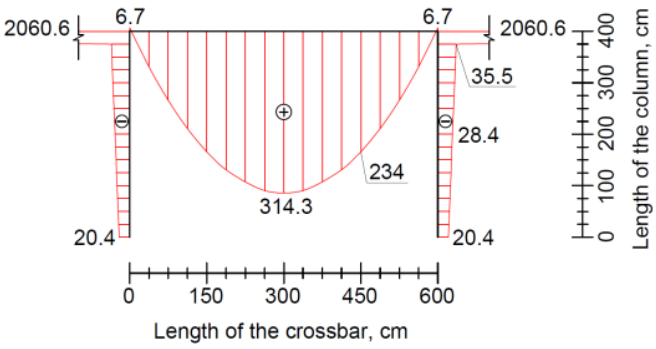

Fig. 18. Distribution of the bimoment (daN ·cm²) with the K_ω = 0.184

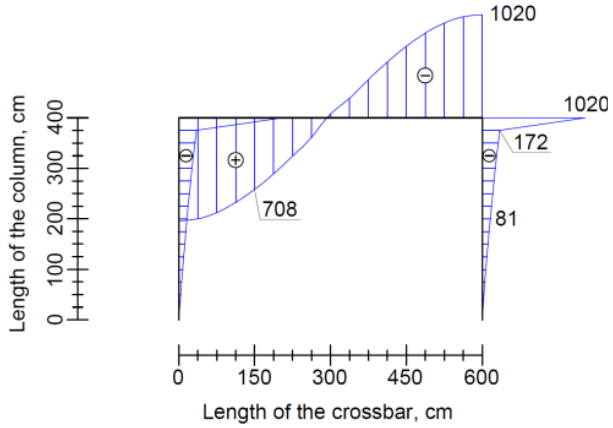

Figure 19. Distribution of the warping (10^{-7} cm^{-1}) without considering the K_ω.

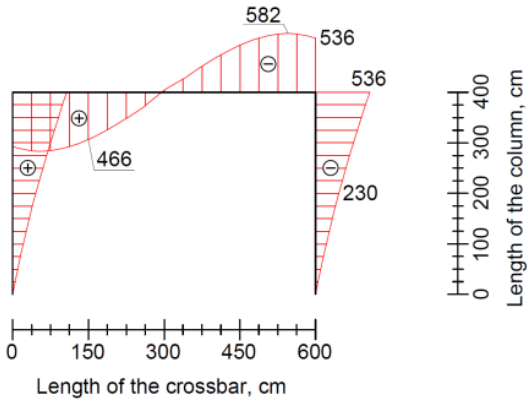

Figure 20. Distribution of the warping (10^{-7} cm^{-1}) with the $K_\omega = 0.184$.

Observing the graphs of the distribution of the bimoments (Fig. 18, Fig. 19) it is important to make next notes.

1) Adding moduli of maximum and minimum values of the bimoment distributed along the crossbar for the calculations with and without the rotation coefficient and equating the obtained values, the next expression is derived:

$$\left(|104.6|+|216.4|\right)\text{daN}\cdot\text{cm}^2=\left(|314.3|+|6.7|\right)\text{daN}\cdot\text{cm}^2$$

$$321\,\text{daN}\cdot\text{cm}^2=321\,\text{daN}\cdot\text{cm}^2 \qquad (4)$$

The identity of the shape and dimensions (4) of the distribution of the bimoment diagrams along the crossbar indirectly confirms the correctness of the obtained results.

2) Comparing the maxima of the bimoments distributed along the crossbar for the calculations with and without the rotation coefficient, one is observed that the maximum value of the bimoment for the calculation considering the rotation coefficient is 31 % higher than the maximum value without considering the rotation coefficient (5).

$$216.4\,\text{daN}\cdot\text{cm}^2<314.3\,\text{daN}\cdot\text{cm}^2 \qquad (5)$$

Such a difference in the obtained results (5) may affect the correctness of the calculated strength of the structure.

4. Conclusion

1. The Tusnin theory of the warping identity of all intersecting in a joint bars does not apply to the calculation of the cross-sectional axis rotation of the thin-walled profiles.

2. The values of normal stresses and the corresponding bimoments are changed considerably with the rotation of the cross-sectional axis (4.3–5.8 times).

3. The coefficient of the cross-sectional axis rotation linearly depends on the change of the geometric parameters of the connecting plate.

4. The change of the thickness of thin-walled profiles negligibly contributes to the value of the coefficient of rotation of the cross-sectional axis.

5. For the observed rigid connection the value of the bimoment with the consideration of the coefficient of the rotation along the column length is 2.86 times reduced in comparison to the calculation without the rotation coefficient. At the same time the value of the bimoment in the joint directly increases by 19.7 times.

6. The maximum value of the bimoment with the consideration of the coefficient of the rotation along the crossbar length is 1.45 times bigger than the one obtained without considering the rotation coefficient.

7. The shape and the dimensions of the distribution of the bimoment diagrams along the crossbar are identical for the calculation with and without the rotation coefficient, which confirms the correctness of the calculations.

References

1. Rybakov, V., Sovetnikov, D., Jos, V. Cross-Sectional Warping of Thin-Walled Rods at Plane Frame Joints. Proceedings of EECE 2019. Lecture Notes in Civil Engineering. 2020. Vol. 70. Pp. 241–243. DOI: 10.1007/978-3-030-42351-3_20
2. Slivker, V.I. Stroitelnaya mekhanika. Variatsionnye osnovy. [Structural mechanics. Variational basis]. Moscow: ASV, 2005. 710 p. (rus)
3. Lalin, V., Rybakov, V., Sergey, A. The finite elements for design of frame of thin-walled beams. Applied Mechanics and Materials. 2014. Vol. 578-579. Pp. 858–863.
4. Lalin, V.V., Rybakov, V.A., Diakov, S.F., Kudinov, V.V., Orlova, E.S. The semi-shear theory of V.I. Slivker for the stability problems of thin-walled bars. Magazine of Civil Engineering. 2019. 87(3). Pp. 66–79. DOI: 10.18720/MCE.87.6
5. Crisfield, M.A. Non-linear Finite Element Analysis of Solids and Structures. Vol. 2. Wiley: Chichester, 1977.
6. Lalin, V.V., Zdanchuk, E.V., Kushova, D.A., Rozin, L.A. Variational formulations for non-linear problems with independent rotational degrees of freedom. Magazine of Civil Engineering. 2015. 56(4). Pp. 54–65. (rus). DOI: 10.5862/MCE.56.7
7. Tusnina, O. A finite element analysis of cold-formed Z-purlins supported by sandwich panels. Applied Mechanics and Materials. 2014. Vol. 467. Pp. 398–403.
8. Tusnina O. An influence of the mesh size on the results of finite element analysis of Z-purlins supported by sandwich panels. Applied Mechanics and Materials. 2014. Vol. 475–476. Pp. 1483–1486.
9. Hsiao, K.M., Lin, J.Y., Lin, W.Y. A consistent co-rotational finite element formulation for geometrically nonlinear dynamic analysis of 3-D beams. Computer Methods in Applied Mechanics and Engineering. 1999. 169 (1). Pp. 1–18.
10. Kibkalo, A., Lebedeva, M., Volkov, M. Methods of Parametric Optimization of Thin-Walled Structures and Parameters which Influence on it. MATEC Web of Conferences 53. 2016. No. 01051.
11. Degtyarev, V.V., Degtyareva, N.V. Finite element modeling of cold-formed steel channels with solid and slotted webs in shear. Thin-Walled Structures. 2016. Vol. 103. Pp. 183–198. DOI: 10.1016/j.tws.2016.02.016
12. Degtyarev, V.V., Degtyareva, N.V. Numerical simulations on cold-formed steel channels with longitudinally stiffened slotted webs in shear. Thin-Walled Structures. 2018. Vol. 129. Pp. 429–546. DOI: 10.1016/j.tws.2018.05.001
13. Degtyarev, V.V., Degtyareva, N.V. Numerical simulations on cold-formed steel channels with flat slotted webs in shear. Part I: Elastic shear buckling characteristics. Thin-Walled Structures. 2017. Vol. 119. Pp. 22–32. DOI: 10.1016/j.tws.2017.05.026
14. Degtyarev, V.V., Degtyareva, N.V. Numerical simulations on cold-formed steel channels with flat slotted webs in shear. Part II: Ultimate shear strength. Thin-Walled Structures. 2017. Vol. 119. Pp. 211–223. DOI: 10.1016/j.tws.2017.05.028
15. Basaglia, C., Camotim, D., Silvestre, N. GBT-based local, distortional and global buckling analysis of thin-walled steel frames. Thin-Walled Structures. 2009. Vol. 47. Pp. 1246–1264. DOI: 10.1016/j.tws.2009.04.003
16. Basaglia, C., Camotim, D., Silvestre, N. Global buckling analysis of plane and space thin-walled frames in the context of GBT. Thin-Walled Structures. 2008. Vol. 46. Pp. 79–101. DOI: 10.1016/j.tws.2007.07.007
17. Basaglia, C., Camotim, D., Silvestre, N. Post-buckling analysis of thin-walled steel frames using generalised beam theory (GBT). Thin-Walled Structures. 2013. Vol. 62. Pp. 229–242. DOI: 10.1016/j.tws.2012.07.003
18. Manta, D., Gonçalves, R., Camotim, D. Combining shell and GBT-based finite elements: Linear and bifurcation analysis. Thin-Walled Structures. 2020. Vol. 152. 106665. DOI: 10.1016/j.tws.2020.106665
19. Pignataro, M., Rizzi, N., Ruta, G., Varano, V. The effects of warping constraints on the buckling of thin-walled structures. Journal of Mechanics of Materials and Structures. 2009. Vol. 4. Pp. 1711–1727. DOI: 10.2140/jomms.2009.4.1711
20. Atavin, I.V., Melnikov, B.E., Semenov, A.S., Chernysheva, N.V., Yakovleva, E.L. Influence of stiffness of node on stability and strength of thin-walled structure. Magazine of Civil Engineering. 2018. 80(4). Pp. 48–61. DOI: 10.18720/MCE.80.5
21. Garifullin, M., Pajunen, S., Mela, K., Heinisuo, M., Havula, J. Initial in-plane rotational stiffness of welded RHS T joints with axial force in main member. Journal of Constructional Steel Research. 2017 Vol. 139. Pp. 353–362.
22. Garifullin, M., Vatin, N., Jokinen, T., Heinisuo, M. Numerical solution for rotational stiffness of RHS tubular joints. Advances and Trends in Engineering Sciences and Technologies II – Proceedings of the 2nd International Conference on Engineering Sciences and Technologies. 2017. Vol. 165. Pp. 1643–1650.
23. Garifullin, M., Bronzova, M., Pajunen, S., Mela, K., Heinisuo, M. Initial axial stiffness of welded RHS T joints. Journal of Constructional Steel Research. 2019. Vol. 153. Pp. 459-472.
24. Rybakov, V.A., Sergey, A. Mathematical analogy between non-uniform torsion and transverse bending of thin-walled open section beams. Applied Mechanics and Materials. 2015. Vol. 725-726. Pp. 746–751.
25. Horacek, M., Melcher, J., Balazs, I., Pesek, O. On Problem of Torsional Characteristics of Thin-walled Steel Beams with Web Openings. IOP Conference Series: Materials Science and Engineering. 2019. Vol. 471. 052040. DOI: 10.1088/1757-899X/471/5/052040
26. Perelmuter, A., Yurchenko, V. On the issue of structural analysis of spatial systems from thin-walled bars with open profiles. Metal constructions. 2014. Vol. 20. No. 3. Pp. 179–190.
27. Tusnin, A.R. Finite element for numeric computation of structures of thin-walled open profile bars. Metal constructions. 2009. Vol. 15. No. 1. Pp. 73–78.
28. Tusnin, A.R. Features of numerical calculation of designs from thin-walled bars of an open profile. Industrial and Civil Engineering. 2010. No. 11. Pp. 60–63.
29. Rybakov, V.A. Metodi resheniya nauchno-teknicheskih zadach v stroitelstve. Chislennie metodi rascheta tonkostennih sterzhnei. [Methods for solving scientific and technical problems in construction. Numerical methods for calculating thin-walled rods]. Saint Petersburg: SPbPU, 2013. 167 p. (rus)
30. Vlasov, V.Z. Thin-walled elastic beams. Israel Program for Scientific Translation. Jerusalem, 1961. 493 p.

Contacts:

Vladimir Rybakov, fishermanoff@mail.ru

Daniil Sovetnikov, sovetnikov.daniil@gmail.com

Vladislav Jos, jos_vlad@mail.ru